

# A robust IMC approach for stability control of 4WS vehicles

M. Canale and L. Fagiano

**Abstract**—A robust non parametric approach is introduced for stability control of four wheel steer by wire vehicles. A feedback structure which regulates both yaw rate and side-slip angle is considered. The uncertainty arising from the wide range of operating conditions is described by a multiplicative model set. Robust stability and saturation effects of the input variables (i.e. front and rear steering angles) are taken into account by means of enhanced Internal Model Control methodologies. In order to provide suitable references for the controlled variables an adaptive generation scheme is adopted on the basis of the driver's manoeuvre requests. Improvements on understeering characteristics, stability over low friction surfaces, damping properties in impulsive manoeuvres and disturbance rejection are shown through simulation results performed on an accurate 10 degree of freedom nonlinear model.

## I. INTRODUCTION

Vehicle active control systems aim to enhance handling and comfort characteristics ensuring stability in critical situations. In this context, a quite common solution is the employment of a yaw rate feedback by means of suitable yaw moments that can be generated in different ways. In particular, the action of active braking systems is employed in Anti Lock Braking System, Vehicle Dynamic Control and Electronic Stability Program strategies; an electronic controlled superposition of an angle to the steering wheel is used in Front Active Steering methodologies; unsymmetrical force distributions for left-right sides of the rear axle are imposed by means of active differential devices; rear steering angle input is applied in Four Wheel Steering systems (see [1] and the references therein for an extensive summary). As a matter of fact, in emergency situations like braking or turning on low friction surfaces it is needed to avoid too large values of the side-slip angle to enhance vehicle performances (see [2]). Moreover, side-slip angle is related to the stability feelings perceived by the driver, thus improvements on its behaviour correspond to more comfortable driving. Therefore, the employment of a side-slip feedback in addition to the yaw rate loop is justified for vehicle stability control. In this paper, the problem of vehicle stability control is considered for a vehicle equipped with a four wheel steer by wire system. Several solutions have been presented in the last years in the context of four wheel steering (4WS) systems. In particular, in [3], the rear steering angle is commanded on the basis of the front steering angle, in [4] a feedback-feedforward structure is employed to control the rear steering angle while the front steering angle remains under the driver

control. More specifically, the use of 4WS by wire has been considered e.g. in [5], where the proposed control structure is able to decouple the control of lateral acceleration and the yaw rate control, and in [6], where Individual Channel Design techniques have been used to design yaw rate and side-slip angle feedbacks. A common problem to all 4WS solutions is the fact that the values of both the input and rear steering angles are subject to physical constraints causing the saturation of the input variables with possible deteriorations of the control performances. An analysis of the saturation effects on the stability performances has been introduced in [6]. In addition, as the vehicle operates under a wide range of conditions of speed, load, friction etc., the active control system has to guarantee safety (i.e. stability) performances robustly in face of the uncertainty arising from such operating situations. Robustness of active vehicle systems is a widely studied topic and interesting results have recently appeared in both parametric and non parametric contexts (see e.g. [7], [8], [9] and [10]).

Therefore, the designer of the control system has to take care of both robust stability and control saturation aspects. As to the choice of the control structure to be adopted a yaw rate plus side-slip angle multivariable feedback has been considered. Internal Model Control (IMC) techniques are used in the design of the feedback controller as they are well established control methodologies able to handle in an effective way both robustness (see [11]) and saturation (see e.g. [12]) issues. In particular, the enhanced IMC structure presented in [13], which guarantees robust stability as well as improved performances during saturation, will be employed. As such design methodology is based on robust  $H_\infty$  optimization techniques, a linear model of the lateral vehicle dynamics will be considered and an unstructured uncertainty description approach will be adopted to take into account the different operating conditions of the vehicle. In order to show in a realistic way the effectiveness of the proposed control approach, simulations will be performed using a detailed nonlinear 10 degrees of freedom vehicle model of an Alfa Romeo segment E car, which proved to give an accurate description of the vehicle dynamics as compared with actual vehicle measurements. Actuator dynamics effects have been included too. The objective of this paper is to show the potentiality of the proposed approach which takes robustly into account both stability and saturation effects. It is assumed that both yaw rate and side-slip angle are measured; however, it is a well known fact that the estimation of the side-slip angle is a quite critical issue. On the other hand, quite good and accurate solutions have been proposed in the literature (see e.g. [2], [14] and [15]) ensuring the reliability of suitable control techniques involving side-slip angle loops.

This research was supported by funds of Ministero dell'Istruzione dell'Università e della Ricerca under the Projects "Advanced control and identification techniques for innovative applications" and "Control of advanced systems of transmission, suspension, steering and braking for the management of the vehicle dynamics".

The authors are with the Dipartimento di Automatica e Informatica, Politecnico di Torino, Corso Duca degli Abruzzi 24 - 10129 Torino - Italy  
e-mail addresses: massimo.canale@polito.it,  
lorenzo.fagiano@polito.it.

## II. PROBLEM FORMULATION

Vehicle stability control aims to change steady state and transient behaviour of the car, enhancing handling performances in turning manoeuvres and keeping safety in presence of unusual external conditions and inputs, such as handwheel steps needed to avoid obstacles, braking under different left-right side adhesion conditions and lateral wind forces. The considered vehicle is equipped with a four wheel steer by wire system thus the control inputs are the front and the rear steering angles  $\delta_f$  and  $\delta_r$  respectively. Therefore, the handwheel angle  $\delta$  issued by the driver is not directly transmitted to the wheels but it is used to describe her/his driving intention in the reference generation design as will be explained in Section IV. The controlled variables are vehicle yaw rate  $\dot{\psi}(t)$  and sideslip angle  $\beta(t)$  as they allow to take into account vehicle safety requirements as well as improvements over the driver stability feeling (see [1]). In order to define the vehicle steady state (i.e. constant speed) requirements in turning manoeuvres we recall that the lateral acceleration  $a_y$  is proportional to the yaw rate through the vehicle speed  $v$ :  $a_y(t) \approx v\dot{\psi}(t)$  (see e.g. [1]). For each constant speed value, by means of standard steering pad manoeuvres it is possible to obtain the steady state lateral acceleration corresponding to different values of the handwheel angle. These values can be graphically represented on the vehicle *understeering* curve (see Figure 1.a) where the handwheel angle is reported with respect to the lateral acceleration. Such curves are mostly influenced by road friction and depend on the tyre lateral force-slip characteristics. An external torque acting on the car centre of gravity is able to vary, under the same steering conditions, the behavior of  $a_y$ , improving the vehicle maximum lateral acceleration and modifying the understeering curve slope according to some desired requirements. The enhancements obtained by the intervention of an additional yaw moment can be described by means of an improved understeering curve (as shown in Figure 1.a, solid line), which can be considered as a target performance to be obtained by the control system. More details about the definition of such target understeering curves will be reported in Section IV. In particular, it will be shown how suitable yaw rate references can be generated on the basis of the desired understeering performances.

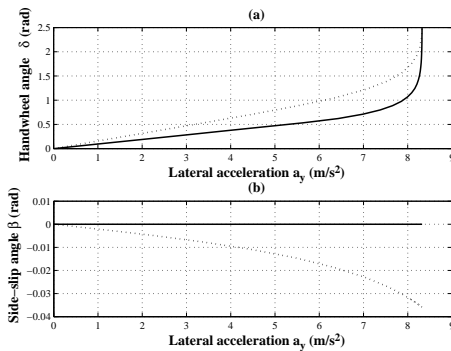


Fig. 1. Uncontrolled vehicle (dotted lines), and target a) yaw rate and b) side-slip angle curves. Vehicle speed: 100 km/h

As regards the desired side-slip angle behaviour a similar

approach could be followed using side-slip curves (i.e.  $\beta$  vs.  $a_y$ ) as depicted in Figure 1.b. In particular, as the smaller the side-slip angle the more comfortable are the turning manoeuvres, the objective to keep as low as possible (namely zero) its value as shown in Figure 1.b. The design of a suitable side-slip reference is shown in Section IV

Therefore improvements on the understeering and side-slip performances may be obtained using suitable modifications of the vehicle lateral dynamics in steady state conditions. A reference generator will provide the (steady state) values for the controlled variables needed to achieve the desired performances by means of a feedback control law. As a matter of fact also in critical manoeuvring situations such as fast path changing at high speed or braking and steering with low and non uniform road friction the vehicle dynamics need to be improved in order to enhance stability and handling performances. In particular, given the swiftness of such manoeuvres the transient vehicle behaviour needs to satisfy good damping and readiness properties. This can be taken into account by the feedback design imposing closed loop bandwidth and well damped closed loop characteristics. Needless to say that at least safety (i.e. stability) requirements have to be guaranteed in face of the uncertainty arising from the wide range of the vehicle operating conditions of speed, load, tyre, friction etc.. This can be achieved by performing a robust controller design using an appropriate description of the uncertainty as it will be described in the following Sections III and IV. Moreover, in order take into account the effects of the input variables saturation (i.e. the maximum allowed values for  $\delta_f$  and  $\delta_r$ ), the controller structure should be provided by suitable implementation solutions like anti-windup schemes to improve the system performances in such situation.

## III. MODEL DESCRIPTION

A standard single track vehicle model (see e.g. [1]) has been used to describe the vehicle dynamics. The dynamic generation mechanism of tyre forces is also modelled by introducing tyre lateral relaxation lengths. The model equations are the following:

$$\begin{aligned} mv(t)\dot{\beta}(t) + mv(t)\dot{\psi}(t) &= F_{yf,p}(t) + F_{yf,p}(t) \\ J_z\ddot{\psi}(t) &= aF_{yf,p}(t) - bF_{yr,p}(t) \\ F_{yf,p}(t) + l_f/v\dot{F}_{yf,p}(t) &= -c_f(\beta(t) + a\dot{\psi}(t)/v(t) - \delta_f(t)) \\ F_{yr,p}(t) + l_r/v\dot{F}_{yr,p}(t) &= -c_r(\beta(t) - b\dot{\psi}(t)/v(t) - \delta_r(t)) \end{aligned} \quad (1)$$

where  $m$  is the vehicle mass,  $J_z$  is the moment of inertia around the vertical axis,  $l$  is the wheel base,  $a$  and  $b$  are the distances between the center of gravity and the front and rear axles respectively; the front and rear tyre relaxation lengths are indicated as  $l_f$  and  $l_r$ , while the symbols  $c_f$  and  $c_r$  stand for the front and rear axle cornering stiffnesses.  $F_{yf,p}$  and  $F_{yr,p}$  are the front and rear axle lateral forces.

Using equations (1), the vehicle yaw rate dynamics can be described by the following transfer matrix  $G$  in the Laplace domain:

$$\begin{bmatrix} \dot{\psi}(s) \\ \beta(s) \end{bmatrix} = \underbrace{\begin{bmatrix} G_{\delta_f, \dot{\psi}}(s) & G_{\delta_r, \dot{\psi}}(s) \\ G_{\delta_f, \beta}(s) & G_{\delta_r, \beta}(s) \end{bmatrix}}_{G(s)} \begin{bmatrix} \delta_f(s) \\ \delta_r(s) \end{bmatrix} \quad (2)$$

Transfer matrix  $G(s)$  will be used in the design of the feedback controller. As already remarked, the real vehicle behaviour is influenced by several different factors that introduce model uncertainty. Therefore, in order to perform a robust design, a multiplicative output uncertainty linear model set of the form (3) has been employed in the control design:

$$\mathcal{G}(G, \Gamma) = \{G(s)(I + \Delta(s)) : \bar{\sigma}(\Delta(\omega)) \leq \Gamma(\omega)\} \quad (3)$$

Such model set has been obtained taking into account the effects of different vehicle speeds ( $\pm 20\%$  of the nominal value) and vehicle inertial characteristics ( $\pm$  to 10% of the nominal mass with consequent geometrical parameters changes). A description of  $\bar{\sigma}(\Delta(\omega))$  obtained by gridding on the considered model parameter variations is reported in Figure 5 of Section V (see [16]).

Finally, in order to compute the reference values for yaw rate and side-slip angle, a single track nonlinear static model is also considered in this paper. Such a model is described in [17] and takes into account the nonlinear axle slip-lateral force relationship introduced in [18]. The single track nonlinear static model equations are of the form:

$$\begin{aligned} m v \dot{\psi} &= F_{yf,p}(\beta, \dot{\psi}, \delta_f) + F_{yr,p}(\beta, \dot{\psi}, \delta_r) \\ a F_{yf,p}(\beta, \dot{\psi}, \delta_f) - b F_{yr,p}(\beta, \dot{\psi}, \delta_r) &= 0 \end{aligned} \quad (4)$$

Numerical computation of such equations gives any feasible steady state motion condition for the nominal vehicle.

#### IV. IMC APPROACH TO STABILITY CONTROL

The considered control structure is depicted in Figure 2. In

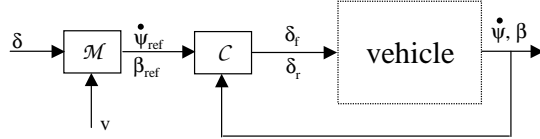


Fig. 2. Considered control structure.

such a structure the desired yaw rate and side-slip angle behaviours are imposed by the reference signals  $\dot{\psi}_{\text{ref}}(t)$ ,  $\beta_{\text{ref}}(t)$  generated by a static map  $\mathcal{M}$  using the values of  $\delta(t)$  and  $v(t)$ . The feedback controller  $\mathcal{C}$  computes the front and rear steering control contributions  $\delta_f(t)$  and  $\delta_r(t)$  needed to follow the required performances described by  $\dot{\psi}_{\text{ref}}(t)$  and  $\beta_{\text{ref}}(t)$ .

##### A. Reference generator

Reference yaw rate and side-slip angle values are generated using a nonlinear static map

$$\begin{bmatrix} \dot{\psi}_{\text{ref}} \\ \beta_{\text{ref}} \end{bmatrix} = f(\delta, v) \quad (5)$$

which uses as input the handwheel angle  $\delta$  imposed by the driver and the vehicle speed  $v$ .  $f(\delta, v)$  is generated according to the control objective, i.e. to keep small side-slip angle values while improving the vehicle understeering curve, in terms of vehicle manoeuvrability and lateral acceleration limit, thus enhancing the overall vehicle handling quality perceived by the driver (see [19]). In order to compute the map values, the single track nonlinear steady state vehicle

model (4) is employed in a three-step procedure. First of all, equations (4) are used to compute any possible controlled vehicle understeering curve, within the vehicle lateral acceleration limit, obtained applying to the front and rear wheels every combination of steering angles inside the saturation limits of the actuators (i.e.  $|\delta_f| \leq 30^\circ$ ,  $|\delta_r| \leq 5^\circ$ ). Thus, for each constant speed value, the working region for the control system can be obtained (see Figure 3, solid lines). This region represents a limit to the reference understeering curve that can be set for the controlled vehicle with the nominal tyre, mass and geometrical characteristics. In the second step, the

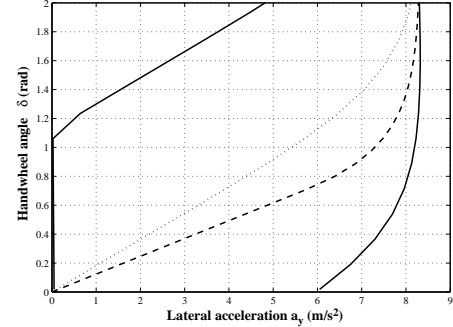


Fig. 3. Control system working region, delimited by solid lines, and uncontrolled (dotted) and reference (dashed) vehicle understeering curves. Speed: 80 km/h

reference understeering curve at each speed value is chosen within the working region according to some performance criteria (e.g. to improve the vehicle manoeuvrability by reducing the slope of the curve for small values of lateral acceleration). To this end, the understeering curve can be divided into a linear tract (i.e. small lateral acceleration values) and into a nonlinear one. In the first tract, the uncontrolled car behaviour can be expressed as:

$$\frac{\delta}{\tau} = \left( \frac{l}{v^2} + K_V \right) a_y = \left( \frac{l}{v} + K_V v \right) \dot{\psi} \quad (6)$$

Where  $\tau$  is the steering wheel ratio of the uncontrolled vehicle. The quantity  $K_V$  is the vehicle *understeering gradient*, which is defined as (see [1]):

$$K_V = \frac{m}{l} \left( \frac{b}{c_f} - \frac{a}{c_r} \right) \quad (7)$$

Equation (6) is obtained considering the cornering stiffness for the overall front (rear) axle instead of the single front (rear) wheels. Since the perceived handling quality of a vehicle with a lower understeering gradient is higher, reference curves in the linear tract are chosen by replacing  $K_V$  in (7) with the *desired* understeering gradient  $K_C$  such that  $0 < K_C < K_V$ . Then, in the nonlinear tract of the curve the desired yaw rate values are computed with a logarithmic function of  $\delta$  which smoothly connects the linear tract of the curve with the chosen maximum lateral acceleration value  $\bar{a}_y$ . The latter is selected to slightly increase the maximum lateral acceleration that can be reached as shown in Figure 3 (dashed line), without violating the physical upper bound suggested by [1]:

$$\bar{a}_y \leq 0.85 \mu g \quad (8)$$

where  $\mu$  is the available tyre-road friction and  $g$  is the gravity acceleration. Thus, a reference understeering curve as showed in Figure 3 is computed for each speed value  $v$ , so a map of values of  $\dot{\psi}_{ref}(\delta, v)$  is obtained. For negative values of  $\delta$ , the symmetrical map with respect to the reference yaw rate obtained for positive  $\delta$  values is considered. The third step corresponds to the choice of the reference side-slip angle values  $\beta_{ref}(\delta, v)$ . As the objective is to limit the side-slip angle value during any manoeuvre,  $\beta_{ref}(\delta, v)$  is chosen, for each value of  $\delta$  and  $v$ , as the lowest value of  $\beta$  that can be obtained given the corresponding reference yaw rate value  $\dot{\psi}_{ref}(\delta, v)$  and the saturation limits of the actuators.

### B. IMC controller design

Internal Model Control (IMC) techniques (see [11]) based on  $H_\infty$  optimization are able to satisfy robust stability requirements in presence of input saturation (see e.g. [20], [13]).

However, as discussed in [12], IMC control may deteriorate the system performances when saturation is active even in absence of model uncertainty. In order to improve the performances under saturation an enhanced robust IMC structure based on the anti-windup IMC solutions presented in [21], [12] has been proposed in [13]. The control scheme considered in [13] gives rise to a nonlinear controller made up by the cascade connection of a linear filter  $Q_1(s)$  and a non linear loop  $Q_2$  which replaces the linear controller  $Q(s)$  as shown in Figure4.

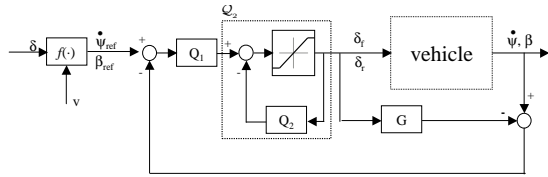


Fig. 4. The proposed control scheme.

In linear operating conditions (i.e. when the saturation is not active) the improved IMC structure is equivalent to a “standard” IMC controller of the form:

$$Q_{eq}(s) = (I + Q_2(s))^{-1} Q_1(s) \quad (9)$$

The design procedure can be summarized in the following steps:

- 1) A preliminary robust IMC controller  $Q(s)$  is computed solving the following optimization problem:

$$\begin{aligned} Q(s) = \\ \arg \min \|W_S^{-1}(s)(I - G(s)Q(s))\|_\infty \\ \text{s.t. } \|\bar{\Gamma}(s)G(s)Q(s)\|_\infty < 1 \end{aligned} \quad (10)$$

where  $\bar{\Gamma}(s)$  is suitable rational function with real coefficients, stable, whose magnitude strictly overbounds the frequency behavior  $\Gamma(\omega)$  and  $W_S(s)$  is a weighting function introduced to take into account a desired specification on the behavior of the sensitivity  $(I - G(s)Q(s))$

- 2) Using controller  $Q(s)$  computed in the previous step, a controller  $Q_2(s)$ , via the design of a preliminary filter  $Q_1(s)$ , is obtained according to the criteria introduced

in [21], [12]. Note that  $Q_2(s)$  must ensure the stability of the non linear loop  $Q_2$  (see Figure 4). To this end, an upper bound  $\gamma_{Q_2}$  on the  $H_\infty$  norm of  $Q_2$  has to be computed (see [13] for details). If  $\gamma_{Q_2}$  is finite then the stability of  $Q_2$  is guaranteed. In case that the stability of  $Q_2$  is not assured then a new controller design has to be performed.

- 3) Then, the linear controller  $Q_1(s)$  can be designed by means of the following  $H_\infty$  optimization problem:

$$\begin{aligned} Q_1(s) = \\ \arg \min \|W_S^{-1}(s)(I - G(s)(I + Q_2(s))^{-1}Q_1(s))\|_\infty \\ \text{s.t. } \|\bar{\Gamma}(s)\gamma_{Q_2}Q_1(s)G(s)\|_\infty < 1 \end{aligned} \quad (11)$$

## V. SIMULATION RESULTS

The control design has been performed using transfer matrix  $G(s)$  defined in (2) computed at a nominal speed  $v = 100 \text{ km/h} = 27.7 \text{ m/s}$  and with the following values of the other involved parameters:

$$\begin{aligned} m &= 1798 \text{ kg} & J_z &= 2900 \text{ kgm}^2 \\ a &= 1.13 \text{ m} & b &= 1.57 \text{ m} \\ l_f &= 0.3 \text{ m} & l_r &= 0.3 \text{ m} \\ c_f &= 76515 \text{ Nm/rad} & c_r &= 96540 \text{ Nm/rad} \end{aligned}$$

The following front and rear wheel steering actuator dynamics have also been considered in control system design and simulations:

$$\begin{aligned} \delta_{f,a}(s) &= \frac{6950}{s^2 + 51s + 6950} e^{-0.02s} \delta_f(s) \\ \delta_{r,a}(s) &= \frac{19290}{s^2 + 85s + 19290} e^{-0.02s} \delta_r(s) \end{aligned} \quad (12)$$

As to the feedback controller design, the desired performance weight to be used in the optimization problems (10) and (12) is described by the function:

$$W_S^{-1}(s) = \frac{s}{s + 20}$$

The computed model uncertainty and weighting function  $\bar{\Gamma}(s)$  are shown in Figure 5

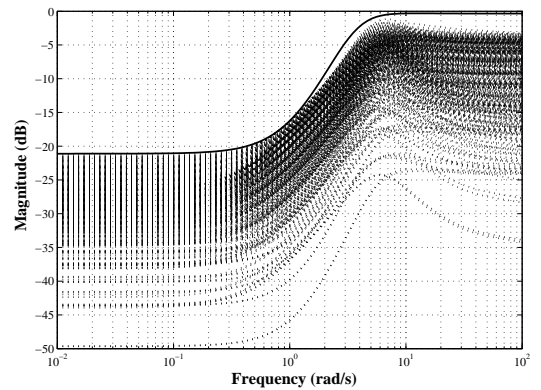


Fig. 5. Model set  $\mathcal{G}$ : multiplicative output uncertainty (dotted) and weighting function  $\bar{\Gamma}(s)$  (solid)

In order to show in a realistic way the performances obtained by the proposed 4WS control approach, simulations have been performed using a detailed nonlinear 10 degrees of freedom Simulink model, validated on the basis of real vehicle measurements. The following open loop (i.e. without driver's feedback) manoeuvres have been chosen to highlight the controlled car safety, as well as steady state and transient handling performances, and to compare these characteristics with the uncontrolled vehicle ones:

- constant speed steering pad performed at 90 km/h: to evaluate steady state vehicle performances, handwheel angle is slowly increased (i.e.  $5^\circ/s$ ) while the vehicle is moving at constant speed, until the vehicle lateral acceleration limit is reached;
- steer reversal test with handwheel angle of  $50^\circ$  performed at 100 km/h, with a handwheel speed of  $400^\circ/s$ . This test aims to evaluate the controlled car transient response performances: in Figure 6 the employed handwheel angle behaviour is showed. To test the control system robustness, the same test has also been performed with a tyre-road friction coefficient  $\mu$  equal to 0.7 (wet road);
- handwheel step input of  $30^\circ$  performed at 70 km/h, with a handwheel speed of  $400^\circ/s$ , and lateral wind disturbance during the cornering, with 100 km/h wind speed. The wind disturbance has been injected after the transient of the reference step input had completed. In this test, vehicle mass was increased by 15%, with consequently changed inertial and geometrical vehicle characteristics. The purpose of this test is to evaluate the control system robustness in front of disturbances and parameter variations.

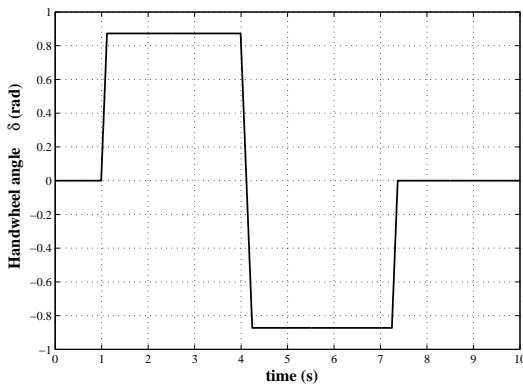


Fig. 6. Handwheel angle input for the steer reversal test

In Figure 7 the understeering and side-slip angle behaviour performance improvement is showed for the considered steering pad manoeuvre. As it can be noted, the target vehicle behaviour in the linear tract, characterized by a lower understeering gradient, is reached while the vehicle side-slip angle value is close to zero. Note that the speed at which the manoeuvre has been performed is different from the nominal speed, thus showing control system robustness.

The  $50^\circ$  steer reversal tests at 100 km/h allow to study the results obtained when the controlled vehicle reaches the yaw rate value of about 0.3 rad/s (see Figure 8), which corresponds to the lateral acceleration limit of about  $8 \text{ m/s}^2$ .

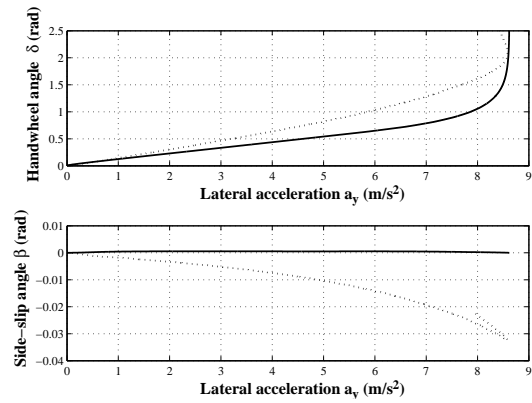


Fig. 7. Comparison between the reference understeering curve (thin solid line) for steering pad manoeuvre at 90 km/h and the ones obtained for the uncontrolled vehicle (dotted) and for the controlled vehicle (solid). In the lower plot, side-slip angle behaviour is reported for the uncontrolled vehicle (dotted line) and for the controlled one (solid line)

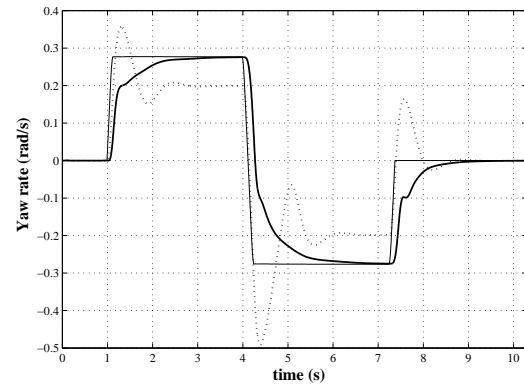


Fig. 8. Steer reversal test: vehicle speed: 100 km/h. Handwheel value:  $50^\circ$ . Comparison between the reference (thin solid line), uncontrolled (dotted) and controlled (solid) vehicle yaw rate

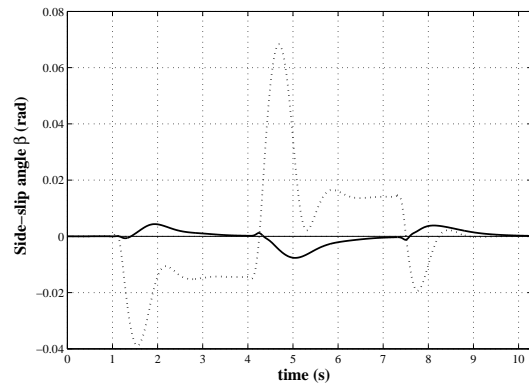


Fig. 9. Steer reversal test: vehicle speed: 100 km/h. Handwheel value:  $50^\circ$ . Comparison between the reference (thin solid line), uncontrolled (dotted) and controlled (solid) vehicle side-slip angle

The yaw rate behavior reported in Figure 8 shows the significant improvements of the system damping properties; at the same time the side-slip angle  $\beta$  (Figure 9) is kept close to zero. Moreover, it can be observed that, according to the target understeering curve, the controlled vehicle reaches a higher lateral acceleration value.

The results of the same test (i.e.  $50^\circ$  at 100 km/h) with low friction coefficient are reported in Figure 10. Note that the control system is not able to reach the reference yaw rate value because of the insufficient friction between the tyres and the ground, since the reference maps has been generated supposing a friction coefficient equal to 1 (dry road). Anyway, the controlled vehicle is able to reach a higher yaw rate value with respect to the uncontrolled vehicle, and the maximum controlled vehicle side-slip angle value  $|\beta(t)|$  obtained during the test is equal to 0.02 rad, while the uncontrolled vehicle reaches a peak of  $|\beta(t)| = 0.09$  rad.

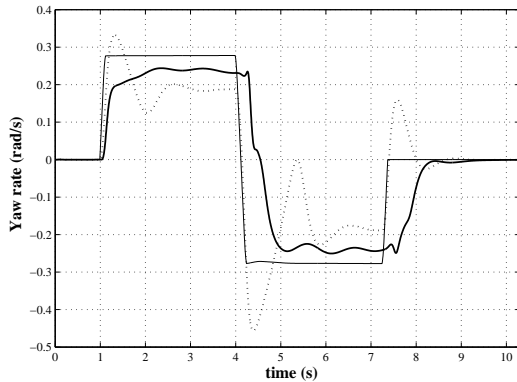


Fig. 10. Steer reversal test at 100 km/h, wet road. Handwheel value:  $50^\circ$ . Comparison between the reference (thin solid line), uncontrolled (dotted) and controlled (solid) vehicle yaw rate

Moreover, the controlled vehicle behaviour obtained during the handwheel step plus wind disturbance test, with increased vehicle mass, shows that the control system is able to reject disturbances and keep stability in presence of parameter variations (see Figure 11)

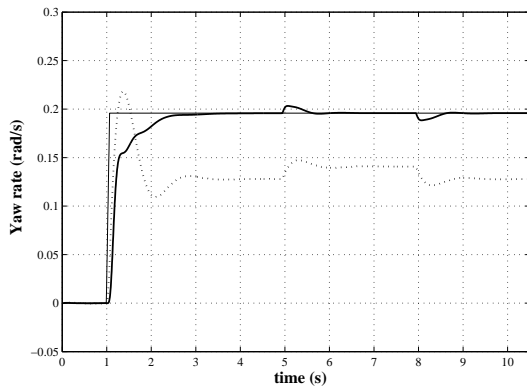


Fig. 11. Handwheel step input of  $30^\circ$  at 70 km/h, with vehicle mass increased by 15%, plus 100 km/h wind disturbance between 5s and 8s. Reference (thin solid line), uncontrolled (dotted) and controlled (solid) vehicle yaw rate

## VI. CONCLUSIONS

A robust non parametric approach to stability control has been presented for four wheel steer by wire vehicles. The proposed control structure exploits the features of Internal Model Control techniques which allow to guarantee robust stability in presence of both model uncertainty and input

saturation. An adaptive generation scheme has been adopted to provide suitable references for the controlled variables according to the driver's manoeuvre requests. Simulation results performed on an accurate vehicle model demonstrate the effectiveness of the employed control strategy. In particular, it has been shown that the achieved performances are very close to the target understeering objectives; a highly damped behaviour in impulsive manoeuvres such as steer reversal tests has been obtained and stability is guaranteed in presence of low friction surfaces in turning manoeuvres and lateral wind disturbances.

## REFERENCES

- [1] R. Rajamani, *Vehicle Dynamics and Control*. Springer Verlag, 2005.
- [2] A. T. V. Zanten, "Bosch ESP systems: 5 years of experience," in *SAE Technical Paper No. 2000-01-1633*, 2000.
- [3] Y. Furukawa, N. Yukara, S. Sano, H. Takeda, and Y. Matsushita, "A review of four wheel steering studies from the viewpoint of vehicle dynamics and control," *Vehicle System Dynamics*, vol. 18, 1989.
- [4] Y. Hirano and K. Fukatani, "Development of robust active rear steering control," in *International Symposium on Advanced Vehicle Control*, 1996.
- [5] J. Ackermann, "Robust decoupling, ideal steering dynamics and yaw stabilization of 4ws cars," *Automatica*, vol. 30, 1994.
- [6] M. A. Vilaplana, O. Mason, D. J. Leith, and W. E. Leithead, "Control of yaw rate and sideslip in 4-wheel steering cars with actuator constraints," *Lecture Notes in Computer Science*, vol. 3355, pp. 201–222, 2005.
- [7] S. Malan, M. Taragna, P. Borodani, and L. Gortan, "Robust performance design for a car steering device," in *33<sup>rd</sup> IEEE Conference on Decision and Control*, 1994.
- [8] J. Ackermann, J. Guldner, R. Steinhausner, and V. I. Utkin, "Linear and nonlinear design for robust automatic steering," *IEEE Trans. on Control System Technology*, vol. 3, no. 1, pp. 132–143, 1995.
- [9] B. A. Güvenç, T. Bünte, and L. Güvenç, "Robust two degree-of-freedom vehicle steering controller design," *IEEE Trans. on Control System Technology*, vol. 12, no. 4, pp. 627–636, 2004.
- [10] J. Gerhard, M.-C. Laiou, M. Mönningmann, W. Marquardt, M. Lakehal-Ayat, and E. A. R. Busch, "Robust yaw control design with active differential and active roll control systems," in *16<sup>th</sup> IFAC World Congress*, Prague, Czech Republic, 2005.
- [11] M. Morari and E. Zafiriou, *Robust Process Control*. Prentice Hall, 1989.
- [12] A. Zheng, M. Kothare, and M. Morari, "Anti-windup design for internal model control," *International Journal of Control*, vol. 60, no. 5, pp. 1015–1022, 1994.
- [13] M. Canale, "Robust control from data in presence of input saturation," *International Journal of Robust and Nonlinear Control*, vol. 14, no. 11, pp. 983–998, 2004.
- [14] J. Ryu and J. C. Gerdes, "Integrating inertial sensors with gps for vehicle dynamics control," *Journal of Dynamic System, Measurements and Control*, 2004.
- [15] D. Piyabongkarn, R. Rajamani, J. A. Grogg, and J. Y. Lew, "Development and experimental evaluation of a slip angle estimator for vehicle stability control," in *American Control Conference*, 2006.
- [16] S. Skogestad and I. Postlethwaite, *Multivariable Feedback Control*. Wiley, 2005.
- [17] M. Canale, L. Fagiano, M. Milanese, and P. Borodani, "Robust vehicle yaw control using an active differential and IMC techniques," *Control Engineering Practice*, 2007.
- [18] E. Bakker, L. Lidner, and H. Pacejka, "A new tyre model with an application in vehicle dynamics studies," in *SAE Paper 890087*, 1989.
- [19] S. Data and F. Frigerio, "Objective evaluation of handling quality," *Journal of Automobile Engineering*, vol. 216, no. 4, pp. 297–305, 2002.
- [20] S. Malan, M. Milanese, D. Regruto, and M. Taragna, "Robust control from data via uncertainty model sets identification," *International Journal of Robust and Nonlinear Control*, vol. 14, no. 11, pp. 945–958, 2004.
- [21] G. Goodwin, S. Graebe, and W. Levine, "Internal model control of linear systems with saturating actuators," in *European Control Conference*, Gröningén, Sweden, 1993.